Beta-decay properties of neutron-rich medium-mass nuclei

2016 J. Phys.: Conf. Ser. 724 012044

(http://iopscience.iop.org/1742-6596/724/1/012044)

Beta-decay properties of neutron-rich medium-mass nuclei

Pedro Sarriguren
Instituto de Estructura de la Materia, IEM-CSIC, Serrano 123, E-28006 Madrid, Spain
E-mail: p.sarriguren@csic.es

Abstract. β-decay properties of even-even and odd-A neutron-rich Ge, Se, Kr, Sr, Zr, Mo, Ru, and Pd isotopes involved in the astrophysical rapid neutron capture process are studied within a microscopic proton-neutron quasiparticle random-phase approximation. The underlying mean field is based on a self-consistent Skyrme Hartree-Fock + BCS calculation that includes deformation as a key ingredient. The isotopic evolution of the various nuclear equilibrium shapes and the corresponding charge radii are investigated in all the isotopic chains. The energy distributions of the Gamow-Teller strength, as well as the β-decay half-lives are discussed and compared with the available experimental information. It is shown that nuclear deformation plays a significant role in the description of the decay properties in this mass region. Reliable predictions of the strength distributions are essential to evaluate decay rates in astrophysical scenarios.

1. Introduction

Weak β-decay is a very important mechanism to understand the late stages of the stellar evolution, playing a critical role to determine both the presupernova stellar structure and the nucleosynthesis of heavier nuclei. These processes are dominated by Gamow-Teller (GT) transitions. An accurate understanding of those astrophysical processes requires input from nuclear physics. Since this information cannot be measured directly in exotic nuclei with very short half-lives, the nuclear properties must be estimated by model calculations. Obviously, nuclear physics uncertainties will finally affect the reliability of the description of those astrophysical processes. Particularly interesting from this point of view is the region of medium-mass neutron-rich nuclei that are involved in the rapid neutron capture process (r process). This process is considered as the main nucleosynthesis mechanism responsible for the production of heavy neutron-rich nuclei and for the existence of about half of the nuclei heavier than iron [1, 2].

In this work, we study the GT strength distributions and β-decay half-lives of neutron-rich nuclei calculated within a proton-neutron quasiparticle random-phase approximation (pnQRPA) based on a selfconsistent deformed Hartree-Fock (HF) mean field with Skyrme interactions including pairing correlations and residual separable forces in both particle-hole (ph) and particle-particle (pp) channels. The present nuclear model has been tested successfully reproducing very reasonably the experimental information available on both bulk and decay properties of medium-mass nuclei [3, 4, 5, 6, 7]. The study is focused on neutron-rich isotopes including $^{80-94}$Ge, $^{86-100}$Se, $^{90-104}$Kr, $^{94-108}$Sr, $^{100-116}$Zr, $^{104-120}$Mo, $^{110-124}$Ru, and $^{114-128}$Pd, although in this work we pay special attention to Kr and Sr isotopes.

2. Theoretical approach

The β-decay half-life is obtained by summing all the allowed transition strengths to states in the daughter nucleus with excitation energies lying below the corresponding Q_{β^-} energy, $Q_\beta = Q_{\beta^-} = M(A,Z) - M(A,Z+1) - m_e$, written in terms of the nuclear masses $M(A,Z)$ and the electron mass (m_e), and weighted with the phase space factors $f(Z, Q_\beta - E_{ex})$,

$$T_{1/2}^{-1} = \frac{(g_A/g_V)_{\rm eff}^2}{D} \sum_{0<E_{ex}<Q_\beta} f\left(Z, Q_\beta - E_{ex}\right) B(GT, E_{ex}) \,, \tag{1}$$

with $D = 6200$ s and $(g_A/g_V)_{\rm eff} = 0.77 (g_A/g_V)_{\rm free}$, where 0.77 is a standard quenching factor. The same quenching factor is included in all the figures shown later for the GT strength distributions. The bare results can be recovered by scaling the results in this paper for $B(GT)$ and $T_{1/2}$ with the square of this quenching factor.

The Fermi integral $f(Z, Q_\beta - E_{ex})$ is computed numerically for each value of the energy including screening and finite size effects [8],

$$f^{\beta^\pm}(Z, W_0) = \int_1^{W_0} pW(W_0 - W)^2 \lambda^\pm(Z, W) {\rm d}W \,, \tag{2}$$

with

$$\lambda^\pm(Z, W) = 2(1+\gamma)(2pR)^{-2(1-\gamma)} e^{\mp \pi y} \frac{|\Gamma(\gamma + iy)|^2}{[\Gamma(2\gamma+1)]^2} \,, \tag{3}$$

where $\gamma = \sqrt{1-(\alpha Z)^2}$; $y = \alpha Z W/p$; α is the fine structure constant and R the nuclear radius. W is the total energy of the β particle, W_0 is the total energy available in $m_e c^2$ units, and $p = \sqrt{W^2 - 1}$ is the momentum in $m_e c$ units.

The nuclear structure involved in the weak rates is described within a microscopic deformed pnQRPA based on a selfconsistent mean field obtained from Skyrme (SLy4) Hartree-Fock + BCS calculations. A residual separable interaction in both *ph* and *pp* is added to the mean field and treated within pnQRPA. More details of the calculation can be found in Refs. [9]. The GT strength for a transition from an initial state i to a final state f is given by

$$B_{if}(GT^\pm) = \langle f || \sum_j^A \sigma_j t_j^\pm || i \rangle^2 \,. \tag{4}$$

3. Results and discussion

We can see in Figures 1 and 2 the isotopic evolution of the quadrupole deformations β (upper plots) and r.m.s. charge radii r_c (lower plots) for Kr and Sr isotopes, respectively. The deformation corresponding to the ground state for each isotope is encircled. For Kr isotopes we can see first a shape transition from prolate ($\beta \approx 0.15$) to oblate ($\beta \approx -0.25$) at $A = 92-94$ and a subsequent transition at $A = 96-98$ from oblate to prolate ($\beta \approx 0.35$) shapes. The radii are sensitive to these transitions, although the measured radii [10] seem to favor prolate shapes in the lighter isotopes. Sr isotopes show a clear transition from oblate to strong prolate ($\beta \approx 0.4$) deformations at $A = 96-98$ ($N = 58-60$). This shape transition is well correlated with the change in the trend observed in the charge radii that shows a sizable jump between ^{96}Sr and ^{98}Sr both theoretically and experimentally [10].

In Figure 3 we can see the accumulated GT strength corresponding to the various deformed equilibrium shapes in Sr isotopes. The GT strength is plotted versus the excitation energy of the daughter nucleus below the Q_β energy. In these figures the sensitivity of the distribution to deformation can be clearly appreciated and one can understand that measurements of the GT

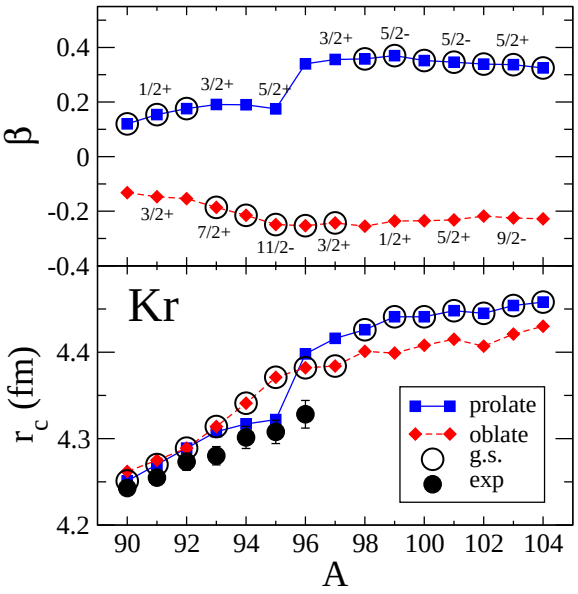

Figure 1. Isotopic evolution of the deformation β and radius r_c in Kr isotopes.

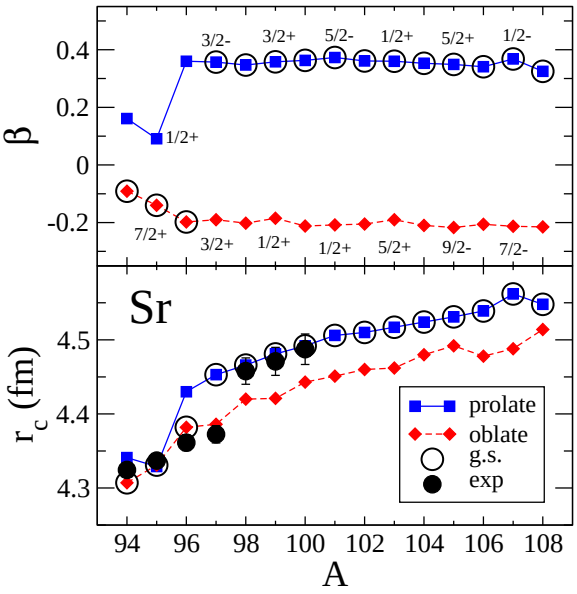

Figure 2. Same as in Fig. 1, but for Sr isotopes.

strength distribution from β-decay can be, in particular cases, an additional source of information about the nuclear deformation, as it was shown in Ref. [3].

The energy distribution of the GT strength is fundamental to constrain the underlying nuclear structure. For a theoretical model, it represents a more demanding test than just reproducing the half-life or the total GT strength that are both integral quantities obtained from these strength distributions properly weighted with phase factors (see Eq. 1) in the case of the half-lives. These quantities might be reproduced even with wrong strength distributions. The calculation of the half-lives in Eq. (1) involves knowledge of the GT strength distribution and of the β energies $(Q_\beta - E_{ex})$, which are evaluated by using Q_β values obtained from the mass differences between parent and daughter nuclei obtained from SLy4.

In Figures 4 and 5 the measured β-decay half-lives, which appear as solid dots (open dots stand for experimental values from systematics) [11, 12], are compared with the theoretical results obtained with the prolate and oblate equilibrium shapes for the Kr and Sr isotopic chains, respectively. For Kr isotopes the general tendency observed experimentally is well reproduced by the calculations, except for the lighter isotopes having larger half-lives. In Sr isotopes the trend observed experimentally is well accounted for, especially with prolate shapes. Half-lives for neutron-rich Kr, Sr, Zr, and Mo isotopes obtained from self-consistent deformed pnQRPA calculations with the Gogny D1M interaction and experimental values of Q_β [13] agree with the results in this work within the uncertainties of the calculations. The agreement is also very reasonable between our calculated half-lives and those obtained from pnQRPA calculations using deformed Woods-Saxon potentials to generate the mean field and complemented with realistic CD-Bonn residual forces [14, 15]. The agreement is also good with the results in Ref. [16] using the Skyrme force SLy4 with fully consistent residual interactions in the *ph* channel.

The impact of deformation on the decay properties is better appreciated by performing a systematic comparison of the half-lives. Figures 6 and 7 show the ratios of the calculated to experimental half-lives for two sets of data corresponding to a spherical calculation (open red dots) and to a deformed calculation at the self-consistent deformation that gives the minimum of the energy (solid black dots). In Figure 6 the ratios are plotted as a function of the quadrupole

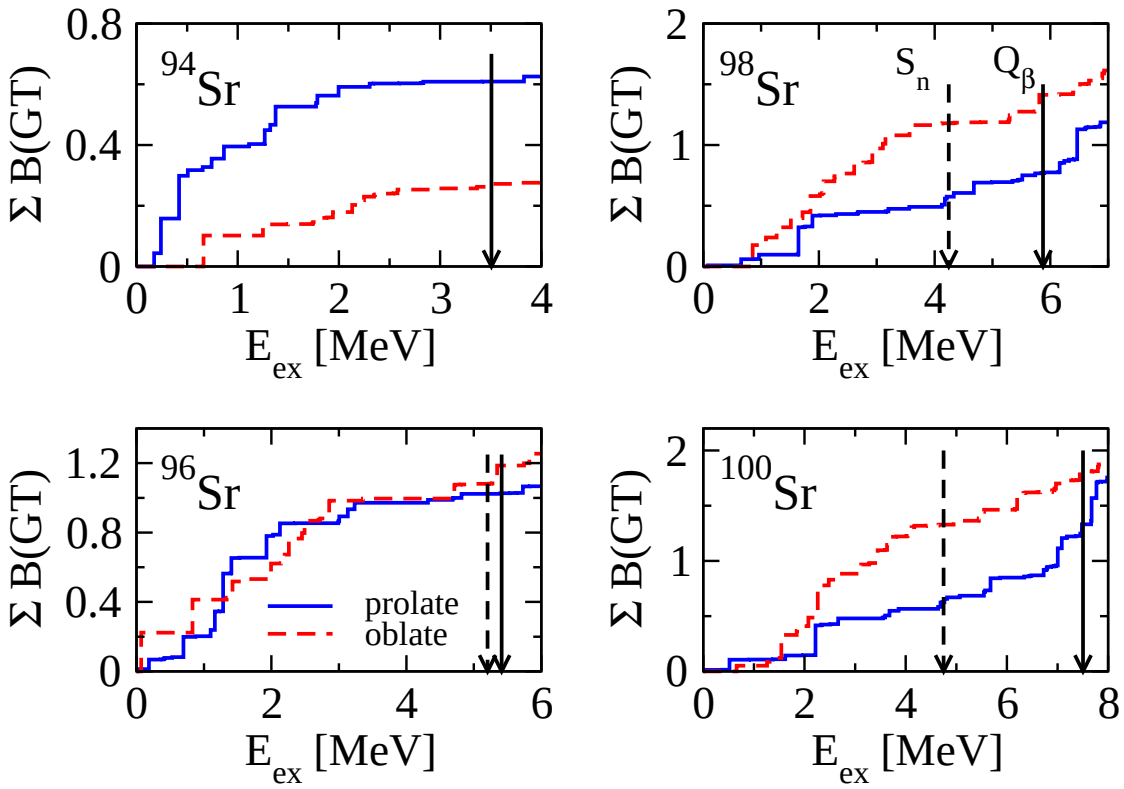

Figure 3. pnQRPA-SLy4 accumulated GT strengths as a function of the excitation energy in the daughter nucleus in some Sr isotopes calculated for the various equilibrium shapes. Q_β and S_n energies are shown by solid and dashed vertical arrows, respectively.

deformation at the minimum of the energy, whereas in Figure 7 the ratios are plotted as a function of the experimental half-lives.

One can see that deformation improves in general the description of the half-lives. Practically all the solid dots are contained within the horizontal lines defining the region of one order of magnitude agreement. On the other hand, the results from the spherical calculation are more spread out with larger discrepancy with experiment.

In order to have a quantitative estimation of the quality of the various calculations, following the analysis made in Ref. [17], the logarithms of the ratios of the calculated and experimental half-lives are introduced through the quantities

$$r = \log_{10}\left[\frac{T_{1/2}(\text{calc})}{T_{1/2}(\text{exp})}\right] . \tag{5}$$

The average position of the points, M_r, and the standard deviation, σ_r, are defined as

$$M_r = \frac{1}{n}\sum_{i=1}^{n} r_i \,; \quad \sigma_r = \left[\frac{1}{n}\sum_{i=1}^{n}(r_i - M_r)^2\right]^{1/2} , \tag{6}$$

and their corresponding factors $M_r^{10} = 10^{M_r}$ and $\sigma_r^{10} = 10^{\sigma_r}$. The analysis of the results involving $n = 81$ nuclei leads to the values $M_r^{10} = 1.105$ and $\sigma_r^{10} = 10.21$ in the spherical case and $M_r^{10} = 0.937$ and $\sigma_r^{10} = 3.09$ in the deformed one. The latter values are clearly closer to unity, showing the improvement achieved with the deformed formalism. Table 1 shows the

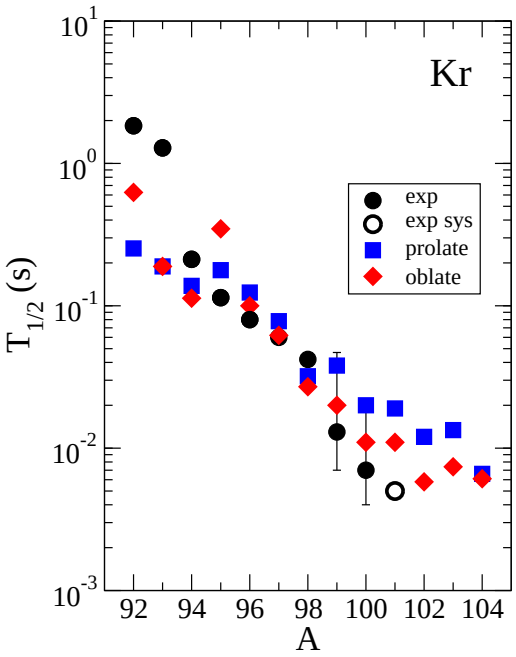

Figure 4. Experimental and calculated half-lives for Kr isotopes.

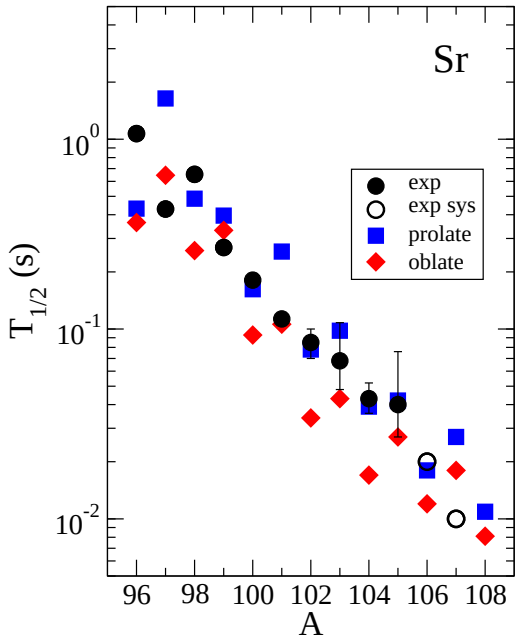

Figure 5. Same as in Fig. 4, but for Sr isotopes.

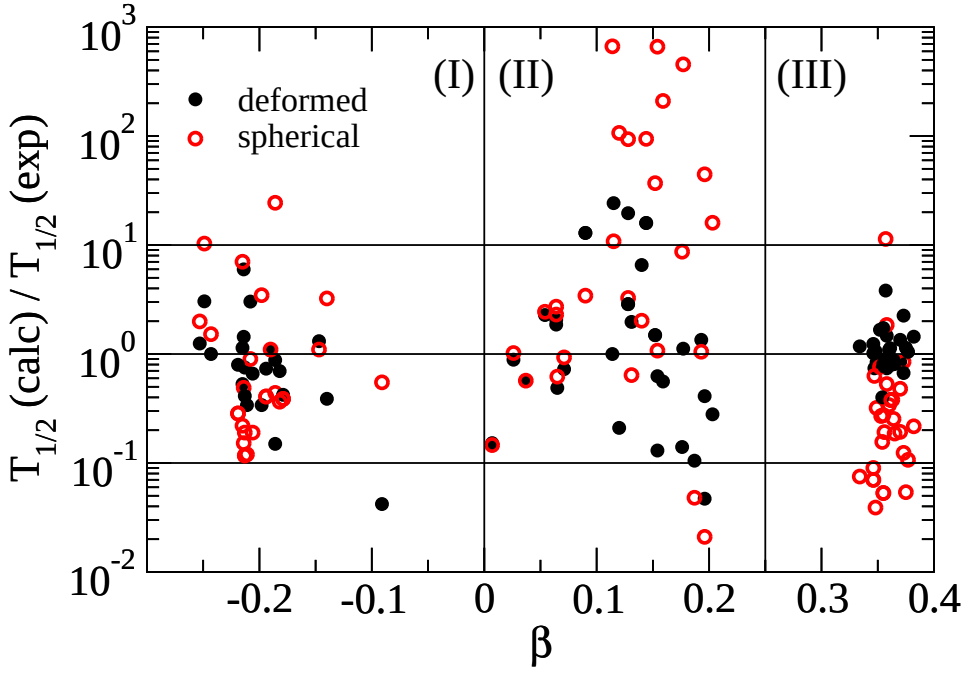

Figure 6.
Ratio of calculated to experimental β-decay half-lives plotted as a function of the quadrupole deformation at equilibrium. The results correspond to spherical (open dots) and deformed (solid dots) calculations.

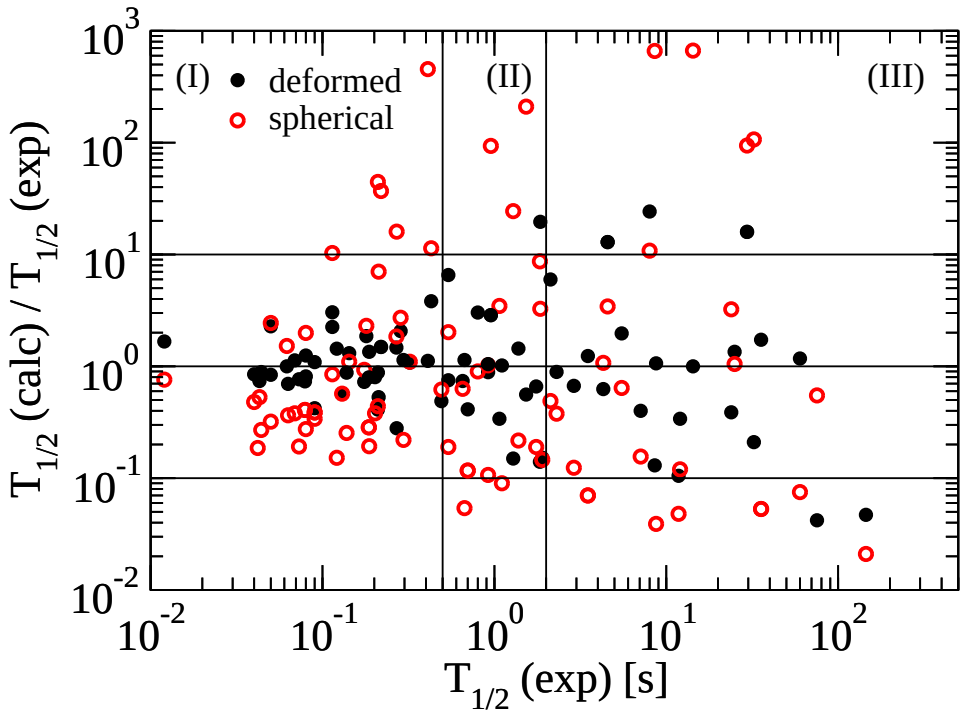

Figure 7.
Same as in Fig. 6, but plotted as a function of the experimental half-lives.

Table 1. Factors of the average position M_r^{10} and standard deviation σ_r^{10} for the ratios r (5) in different regions of half-lives and deformations.

		M_r^{10}	σ_r^{10}	points
Global	sph	1.105	10.213	81
	def	0.937	3.088	
$0.01 < T_{1/2} < 0.5$	sph	1.172	5.691	42
	def	1.053	1.758	
$0.5 < T_{1/2} < 2$	sph	1.078	10.952	18
	def	0.903	3.509	
$2 < T_{1/2} < 500$	sph	1.001	21.473	21
	def	0.843	5.376	
$-0.3 < \beta < 0$	sph	0.898	4.442	25
	def	0.744	2.647	
$0 < \beta < 0.25$	sph	5.662	15.710	28
	def	1.014	5.000	
$0.25 < \beta < 0.40$	sph	0.260	3.285	28
	def	1.062	1.518	

results of this global analysis, as well as the results corresponding to different regions in both half-lives and quadrupole deformations. The improvement of the deformed formalism is evident in the regions of well deformed nuclei and short half-lives, where the large Q_β-values make the

half-lives more significant as they are sensitive to a larger region of the GT strength distribution.

4. Conclusions

We have studied the isotopic evolution of bulk and decay properties of neutron-rich medium-mass nuclei. The nuclear structure involved in the calculation of the energy distribution of the Gamow-Teller strength is described within a selfconsistent deformed HF+BCS+QRPA formalism with density-dependent effective Skyrme interactions and spin-isospin residual interactions. We find that the present pnQRPA calculation is able to reproduce the main features of the decay properties based on the experimental information available on β-decay half-lives. Predictions for the Gamow-Teller strength distributions have been made in the relevant range of energies below the Q_β-windows. A systematic comparison of the ratios of the calculated and experimental half-lives has been done using both spherical and deformed calculations, showing that the inclusion of deformation improves significantly the description of the decay properties.

Acknowledgments

This work was supported in part by MINECO (Spain) under Research Grants Nos. FIS2011–23565 and FIS2014–51971–P.

References

[1] Burbidge EM *et al.* 1959 *Rev. Mod. Phys.* **29** 547
[2] Cowan JJ *et al.* 1991 *Phys. Rep.* **208** 267
[3] Nácher E *et al.* 2004 *Phys. Rev. Lett.* **92** 232501; Poirier E *et al.* 2004 *Phys. Rev.* C **69** 034307; Pérez-Cerdán AB *et al.* 2013 *Phys. Rev.* C **88** 014324
[4] Sarriguren P *et al.* 2003 *Nucl. Phys.* **A716** 230; Sarriguren P 2013 *Phys. Rev.* C **87** 045801
[5] Sarriguren P *et al.* 2005 *Eur. Phys. J.* A **24** 193; Sarriguren P 2009 *Phys. Rev.* C **79** 044315; Sarriguren P 2009 *Phys. Lett.* B **680** 438; Sarriguren P 2011 *Phys. Rev.* C **83** 025801
[6] Sarriguren P and Pereira J 2010 *Phys. Rev.* C **81** 064314; Sarriguren P, Algora A, and Pereira J 2014 *Phys. Rev.* C **89** 034311; Sarriguren P 2015 *Phys. Rev.* C **91** 044304
[7] Sarriguren P *et al.* 2005 *Phys. Rev.* C **72** 054317; Moreno O *et al.* 2006 *Phys. Rev.* C **73** 054302; Boillos JM *et al.* 2015 *Phys. Rev.* C **91** 034311
[8] Gove NB and Martin MJ 1971 *At. Data Nucl. Data Tables* **10** 205
[9] Sarriguren P *et al.* 1998 *Nucl. Phys.* **A635** 55; Sarriguren P *et al.* 1999 *Nucl. Phys.* **A658** 13; Sarriguren P *et al.* 2001 *Nucl. Phys.* **A691** 631; Sarriguren P *et al.* 2001 *Phys. Rev.* C **64** 064306
[10] Angeli I 2004 *At. Data Nucl. Data Tables* **87** 185
[11] Audi G *et al.* 2012 *Chinese Physics* C **36** 1157
[12] Nishimura S *et al.* 2011 *Phys. Rev. Lett.* **106** 052502
[13] Martini M *et al.* 2014 *Phys. Rev.* C **89** 044306
[14] Fang FL *et al.* 2013 *Phys. Rev.* C **88** 024314
[15] Ni D and Ren Z 2014 *Phys. Rev.* C **89** 064320; 2012 *J. Phys. G: Nucl. Part. Phys.* **39** 125105
[16] Yoshida K 2013 *Prog. Theor. Exp. Phys.* 113D02
[17] Moeller P, Pfeiffer B, and Kratz KL 2003 *Phys. Rev.* C **67** 055802